

# Effect of Adipose Tissue-Derived Osteogenic and Endothelial Cells on Bone Allograft Osteogenesis and Vascularization in Critical-Sized Calvarial Defects

Agustin Cornejo, M.D.,<sup>1</sup> David E. Sahar, M.D.,<sup>1</sup> Stacy M. Stephenson, M.D.,<sup>1</sup> Shiliang Chang, M.D.,<sup>1</sup> Son Nguyen, M.D.,<sup>1</sup> Teja Guda, Ph.D.,<sup>2</sup> Joseph C. Wenke, Ph.D.,<sup>2</sup> Amanda Vasquez, B.S.,<sup>1</sup> Joel E. Michalek, Ph.D.,<sup>3</sup> Ramaswamy Sharma, Ph.D.,<sup>4</sup> Naveen K. Krishnegowda, M.D.,<sup>1</sup> and Howard T. Wang, M.D.<sup>1</sup>

The use of processed bone allograft to repair large osseous defects of the skull has been limited, given that it lacks the osteogenic cellularity and intrinsic vascular supply which are essential elements for successful graft healing and, at the same time, the areas to be targeted through tissue-engineering applications. In this study, we investigated the effect of predifferentiated rat adipose tissue-derived osteoblastic cells (OBs) and endothelial cells (ECs) on calvarial bone allograft healing and vascularization using an orthotopic critical-sized calvarial defect model. For this purpose, thirty-seven 8 mm critical calvarial defects in Lewis rats were treated with bone allografts seeded with no cells, undifferentiated adipose tissue-derived stem cells (ASC), OBs, ECs, and OBs and ECs simultaneously. After 8 weeks, the bone volume and mineral density were calculated using microcomputed tomography and the microvessel formation using immunohistochemical staining and imaging software. The amount of bone within the 8 mm defect was significantly higher for the allografts treated with ECs compared with the allografts treated with OBs ( $p=0.05$ ) and simultaneously with the two cell lineages ( $p=0.02$ ). There were no significant differences in bone formation between the latter two groups and the control groups (allografts treated with no cells and undifferentiated ASC). There were no significant differences in bone mineral density among the groups. The amount of microvessels was significantly higher in the group treated with ECs relative to all groups ( $p < 0.05$ ). Our results show that the implantation of ASC-derived ECs improves the vascularization of calvarial bone allografts at 8 weeks after treatment. This cell-based vascularization strategy can be used to improve the paucity of perfusion in allogenic bone implants. However, in this study, the treatment of allografts with OBs alone or in combination with ECs did not support bone formation or vascularization.

## Introduction

THE RESTORATION OF critical-sized osseous defects of the craniofacial skeleton after traumatic injury or surgical resection remains a challenge to the reconstructive surgeon. Whenever possible, these defects are reconstructed with vascularized autologous bone which contains osteogenic cells (osteogenic properties), has chemotactic factors that facilitate the recruitment of osteoprogenitor cells (osteoinductive properties), provides the optimal physical conditions for the bone to regenerate (osteoconductive properties), and has adequate blood supply to support graft viability; characteristics that explain its efficacy for bone reconstruction.<sup>1</sup>

However, harvesting autologous bone is not always feasible, especially when the tissue is limited or when the procedure poses prohibitive health risks for the individual. In these circumstances, the use of processed bone allograft is considered an acceptable substitute.<sup>2</sup> However, its use has been associated with limited graft viability after implantation and also with failure to remodel and incorporate with the host bone, resulting in failure rates of 40% within 10 years, which has halted its widespread use in spite of its ready availability.<sup>3,4</sup> Although allogenic bone preserves its osteoconductive properties after processing, it lacks the osteogenic cells and osteoinductive growth factors needed to synthesize new bone. After implantation, the allograft is slowly resorbed and

<sup>1</sup>Division of Plastic and Reconstructive Surgery, University of Texas Health Science Center at San Antonio, San Antonio, Texas.

<sup>2</sup>Extremity Trauma and Regenerative Medicine Task Area, United States Army Institute of Surgical Research, Houston, Texas.

Departments of <sup>3</sup>Epidemiology and Biostatistics, and <sup>4</sup>Cellular and Structural Biology, University of Texas Health Science Center at San Antonio, San Antonio, Texas.

# Report Documentation Page

Form Approved  
OMB No. 0704-0188

Public reporting burden for the collection of information is estimated to average 1 hour per response, including the time for reviewing instructions, searching existing data sources, gathering and maintaining the data needed, and completing and reviewing the collection of information. Send comments regarding this burden estimate or any other aspect of this collection of information, including suggestions for reducing this burden, to Washington Headquarters Services, Directorate for Information Operations and Reports, 1215 Jefferson Davis Highway, Suite 1204, Arlington VA 22202-4302. Respondents should be aware that notwithstanding any other provision of law, no person shall be subject to a penalty for failing to comply with a collection of information if it does not display a currently valid OMB control number.

|  |                                   |                                    |   |  |                                 |
|--|-----------------------------------|------------------------------------|---|--|---------------------------------|
| 1. REPORT DATE<br><b>01 AUG 2015</b>   |                                   | 2. REPORT TYPE<br><b>N/A</b>       |   | 3. DATES COVERED<br><b>-</b>             |                                 |
| 4. TITLE AND SUBTITLE<br><b>Effect of Adipose Tissue-Derived Osteogenic and Endothelial Cells on Bone Allograft Osteogenesis and Vascularization in Critical-Sized Calvarial Defects</b> |                                   |                                    |   | 5a. CONTRACT NUMBER                      |                                 |
|  |                                   |                                    |   | 5b. GRANT NUMBER                         |                                 |
|  |                                   |                                    |   | 5c. PROGRAM ELEMENT NUMBER               |                                 |
| 6. AUTHOR(S)<br><b>Cornejo A., Sahar D. E., Stephenson S. M., Chang S., Nguyen S., Guda T., Wenke J. C., Vasquez A., Michalek J. E., Sharma R.,</b>                                      |                                   |                                    |   | 5d. PROJECT NUMBER                       |                                 |
|  |                                   |                                    |   | 5e. TASK NUMBER                          |                                 |
|  |                                   |                                    |   | 5f. WORK UNIT NUMBER                     |                                 |
| 7. PERFORMING ORGANIZATION NAME(S) AND ADDRESS(ES)<br><b>United States Army Institute of Surgical Research, JBSA Fort Sam Houston, TX</b>  |                                   |                                    |   | 8. PERFORMING ORGANIZATION REPORT NUMBER |                                 |
| 9. SPONSORING/MONITORING AGENCY NAME(S) AND ADDRESS(ES)  |                                   |                                    |   | 10. SPONSOR/MONITOR'S ACRONYM(S)         |                                 |
|  |                                   |                                    |   | 11. SPONSOR/MONITOR'S REPORT NUMBER(S)   |                                 |
| 12. DISTRIBUTION/AVAILABILITY STATEMENT<br><b>Approved for public release, distribution unlimited</b>  |                                   |                                    |   |  |                                 |
| 13. SUPPLEMENTARY NOTES  |                                   |                                    |   |  |                                 |
| 14. ABSTRACT   |                                   |                                    |   |  |                                 |
| 15. SUBJECT TERMS  |                                   |                                    |   |  |                                 |
| 16. SECURITY CLASSIFICATION OF:  |                                   |                                    | 17. LIMITATION OF ABSTRACT<br><b>UU</b> | 18. NUMBER OF PAGES<br><b>11</b>         | 19a. NAME OF RESPONSIBLE PERSON |
| a REPORT<br><b>unclassified</b>  | b ABSTRACT<br><b>unclassified</b> | c THIS PAGE<br><b>unclassified</b> |   |  |                                 |

simultaneously replaced with new viable bone.<sup>4</sup> This process is called creeping substitution and may involve only 20% of the graft in 5 years, as demonstrated by studies conducted on retrieved allografts.<sup>5</sup> Furthermore, allogenic bone is not vascularized and, thus, relies on the diffusion of oxygen and nutrients from the surrounding blood vessels until a capillary network is established. The diffusion capacity is limited to only 150–200  $\mu\text{m}$ , and, therefore, the paucity of vascularization poses a major limitation to the allograft viability after implantation as well as to their potential size.<sup>6,7</sup>

With the discovery of adipose tissue-derived stem cells (ASC), the field of tissue engineering has become a promising therapeutic strategy that addresses the limitations of allogenic bone reconstruction. Adipose tissue-derived stem cells not only differentiate into osteoblastic cells (OBs) or endothelial cells (ECs), but also are obtainable in large quantities and provide an excellent cellular source for engineered constructs.<sup>8–11</sup> Studies in several animal models have demonstrated that the implantation of osteoprogenitor cells and OBs can improve the osteogenic and osteoinductive potential of allogenic bone, which occurs likely secondary to the production of growth factors and bone morphogenetic proteins (BMPs) that reciprocally stimulate OBs to form mineralized bone matrix.<sup>5,12–15</sup> In addition, in order to improve the blood supply of such grafts, angiogenic strategies have been developed and include the direct application of angiogenic growth factors such as vascular endothelial growth factor (VEGF) and fibroblast growth factor as recombinant proteins or by gene therapeutics.<sup>16,17</sup> However, growth factors are only one of the several factors involved in angiogenesis, which ultimately depends on the migration and formation of endothelial and mural cells.<sup>18</sup> Recently, cell-based therapies using endothelial progenitor cells (EPCs) or ECs have been successful in inducing the formation of microcapillary structures *in vivo* when implanted in a variety of scaffolds.<sup>16,19–22</sup> Given that bone matrix is the most osteoconductive scaffold for tissue-engineering applications,<sup>23</sup> if we can augment the osteogenic potential of allogenic bone by adding OBs and, at the same time ECs, then, we could potentially overcome a main limitation of allogenic bone repair. Therefore, the objective of the present study is to investigate the effect of *in vitro* predifferentiated rat adipose-tissue derived OBs and ECs on bone allograft healing and vascularization using an orthotopic critical-sized calvarial defect model. We hypothesized that treating processed bone allografts with OBs and ECs independently will improve their osteogenic and angiogenic potential, respectively, and (2) that treating bone allografts with OBs and ECs simultaneously will convey a synergistic effect on allograft healing.

## Materials and Methods

### *Adipose-derived stem cell isolation and culture*

The study protocol was approved by the University of Texas Health Science Center at San Antonio Animal Use Committee. Under general anesthesia using isoflurane, adipose tissue excised from the perinephric and peritesticular fat pad of ten 8-week-old Lewis rats was washed with sterile pH balanced Hank's balanced salt solution (HBSS) (Invitrogen), finely minced using sharp dissection, placed in sterile HBSS containing 25 mL of 1% bovine serum albumin (BSA) and 0.075% collagenase (type I; Sigma-Aldrich), and then allowed

to agitate at 37°C for 1 h. An equal volume of Dulbecco's modified Eagle medium and nutrient mixture F-12 media (DMEM/F-12) (Invitrogen) with 10% fetal bovine serum (FBS) (Gibco Invitrogen) was added for collagenase neutralization. The digest was filtered twice through 100  $\mu\text{m}$  nylon mesh cell strainers and centrifuged at room temperature for 5 min at 600 *g*. The supernatant was removed, and the cell pellet was resuspended in media consisting of DMEM/F-12, 10% FBS, 100 U/mL penicillin, and 100  $\mu\text{g}/\text{mL}$  streptomycin (Mediatech; Cellgro). Cell counts were determined with a hemocytometer. The cells were plated in 75  $\text{cm}^2$  vented tissue culture flasks at a density of  $1 \times 10^6$  cells per flask and incubated at 37°C with 5%  $\text{CO}_2$ . The average cell yield was  $1 \times 10^6$  cells/gm of adipose tissue. After isolation, the cells were cultured for a 5–7 day period and were used for differentiation after the third passage.

### *Osteogenic induction and characterization*

After the third passage, the cells were cultured in an osteogenic medium (OM) consisting of DMEM, 10% FBS, 1% penicillin/streptomycin (Mediatech; Cellgro), 0.1  $\mu\text{M}$  dexamethasone, 10 mM  $\beta$ -glycerol phosphate, and 50  $\mu\text{M}$  ascorbic acid; the OM was changed every third day for 21 days. Immunocytofluorescence studies were performed to detect the induced osteoblastic phenotypes. The induced OBs were fixed in 4% paraformaldehyde, permeated with 0.2% Tween in phosphate-buffered saline, and incubated in 1% BSA and 10% goat serum for 1 h at 37°C. A primary antibody to osteocalcin was then added in blocking solution (sc-23790; Santa Cruz Biotech), and cells were maintained at 4°C overnight. The bound antibodies were detected by incubation for 1 h at 37°C with a secondary antibody conjugated to Alexa 488 fluorochrome (A11055; Invitrogen) along with Hoechst 33258 (Invitrogen). The cells were visualized in an Olympus FV1000 confocal microscope (Olympus). Images were sequentially acquired and analyzed using FV10-ASW version 2.1.

The presence of calcium deposits was demonstrated by von Kossa staining. After fixation in 3.7% paraformaldehyde (Sigma) for 30 min, the cells were incubated with 5% silver nitrate solution (Gibco) under ultraviolet light for 60 min.

### *Endothelial induction and characterization*

After the third passage, the cells were cultured in a vasculogenic medium consisting of DMEM, 10% FBS, 1% penicillin/streptomycin, and 50 ng/mL recombinant rat VEGF-C (Promocell, Heidelberg, Germany). The media were changed every other day for 8 days before implantation in the bone allografts. The VEGF-C was added fresh to stock media before each media change. Immunocytofluorescence studies were performed to detect the induced endothelial phenotypes. After fixation, permeation, and blocking as previously described, the primary antibody to CD31 (MAB1393; Millipore, Billerica, MA) was added to the cells at 4°C overnight. The bound antibodies were detected by incubation for 1 h at 37°C with the secondary antibody conjugated to Alexa 568 (A11036 or A11004; Invitrogen) along with Hoechst 33258 (Invitrogen). The cells were visualized in an Olympus FV1000 confocal microscope (Olympus). The images were sequentially acquired and analyzed using FV10-ASW version 2.1.

### *Bone allograft construct preparation and implantation*

Eight-millimeters $\times$ 2-mm sterilized and decellularized banked allografts from previously harvested Lewis rat calvaria were used for the bone constructs. In order to sterilize and decellularize the grafts, these were soaked in a 0.5 mg/mL gentamicin solution for 30 min, sonicated for 30 min, then incubated in a 70% ethanol for one hour, and allowed to air dry in a laminar flow hood for graft sterilization. Before implantation, the processed bone constructs were placed into 24-well plates containing 1 mL of different media according to the anticipated treatment group: OM, endothelial media (EM), a 1:1 mixture of OM and EM, and DMEM-F12 medium (Invitrogen) and incubated at 37°C with 5% CO<sub>2</sub> for 2 days. At the time of seeding, the cells were resuspended to a concentration of 20,000 cells/ $\mu$ L before being added drop wise to the bone allograft surface. A total of  $2\times 10^5$  second passage ASC and predifferentiated OBs and ECs were seeded onto the allografts independently. When OBs and ECs were co-seeded, a total of  $1\times 10^5$  cells of each cell lineage were implanted (1:1 cell ratio). The cells were allowed to incubate for 30 min at 37°C with 5% CO<sub>2</sub> before adding 500  $\mu$ L of the respective culture media to each well, followed by incubation at 37°C with 5% CO<sub>2</sub> for 2 days. Subsequently, the rat calvarias were exposed using a midline scalp incision, and the skin and periosteum were laterally reflected. An 8-mm defect was created using an 8-mm trephine burr, leaving the dura mater intact. The allograft construct was implanted into the calvarial defect, and the scalp was approximated using absorbable sutures. The critical-sized calvarial defects were treated with the bone allografts previously seeded with (1) no cells ( $n=10$ ); (2) undifferentiated ASC ( $n=10$ ); (3) adipose tissue-derived OBs (Osteo,  $n=10$ ); (4) adipose tissue-derived ECs (Endo,  $n=10$ ); and (5) adipose tissue-derived OBs and ECs simultaneously (Osteo-Endo,  $n=10$ ). At 8 weeks postoperatively, the rats were euthanized, and their calvaria were harvested for radiographic and histological examination.

### *Microcomputed tomography analysis*

The samples were scanned using microcomputed tomography ( $\mu$ CT) SkyScan 1076 (Skyscan) at a 100 kV source voltage and a 100  $\mu$ A source current with no filter used and at a spatial resolution of 8.77  $\mu$ m. The reconstructions were performed using NRecon software (Skyscan), and this resulted in grayscale images that spanned a density range from 0.96 to 2.57 g/cm<sup>3</sup> corresponding to gray scale values from 0 to 255. DataViewer (Skyscan) was used to reslice the  $\mu$ CT images along coronal and sagittal axes that were used to reorient the  $\mu$ CT slices to be perpendicular to the cranial-caudal axis of the calvaria, and  $\mu$ CT thresholding was performed to include only ossified tissues. The thresholds were selected as the histogram minima between the peaks representing the formalin in which the sample was scanned and the bone volume of the sample. The geometric mean of the threshold for all 100 samples in the study was used to determine the upper and lower threshold for binarization as 32 and 250. The region of interest (ROI) was chosen by creating a volume that spanned 8 mm around the defect generated in the calvaria and repaired with allograft to include the entire defect generated. Additional analyses were performed by choosing concentric ROI 7 mm and 9 mm in di-

ameter as well as the remainder of the native calvaria. All ROI comprised the full thickness of the calvaria. Since there is no discernible difference between the density of implanted allograft and regenerated bone, these could not be distinguished independently and are reported as total ossified tissues within the defect. The total volume of bone in this three-dimensional (3D) volume was computed using CTAn software (Skyscan) from the binarized data. The mean bone density of the ossified tissues within these 3D volumes were calculated before binarization as the mean grayscale value of all pixels between the chosen thresholds.

### *Histological evaluation of vascularization*

After  $\mu$ CT, the specimens were fixed in 10% neutral phosphate-buffered solution formalin, demineralized in ethylenediaminetetraacetic acid solution, dehydrated in a series of alcohol washes, and embedded in paraffin. The specimens were sectioned in the coronal plane in the center of the bone scaffolds at a thickness of 6  $\mu$ m and stained with hematoxylin and eosin for visualization through conventional qualitative bright-field microscopy analysis. For quantification of blood vessels, three sections per animal stained with a rat-specific anti-CD34 antibody (R&D Systems AF4117/Goat pAb) and counterstained with hematoxylin were analyzed. Microscopic pictures were randomly taken at 10-fold magnification including three central and three peripheral areas per section for a total of six pictures. To determine the microvascular density (mean number of capillaries per mm<sup>2</sup>), the number of structures with lumen surrounded by CD34-positive cells was manually counted. A histomorphometric analysis of the tissue area on the pictures was performed using Image J (NIH). Image collection and quantification were performed by one author blinded to the treatment groups.

### *Statistical analysis*

Analysis of variance with a Tukey correction for multiple comparisons using Statistical Analysis Software (SAS Institute) was performed for all acquired  $\mu$ CT and microvessel quantification data. All data are presented as the mean  $\pm$  standard deviation. In all statistical evaluations,  $p < 0.05$  was considered statistically significant.

## **Results**

### *Cell culture and characterization*

The cell colonies incubated in osteogenic or endothelial medium were observed after the primary passage. The differentiating cells established specific morphologies; cells in OM displayed an osteoblast-like spindle morphology (Fig. 1A), and cells in endothelial medium displayed a characteristic cobblestone morphology (Fig. 1B). Osteoblast calcium mineral deposition was observed as darkly stained mineralized nodules with von Kossa staining, indicating normal osteoblast function in a conditioned culture (Fig. 1C). In addition, the capacity of the osteogenic-wise induced cells to express osteocalcin was demonstrated by immunocytofluorescence (Fig. 1D). The differentiation ability of ECs induced from adipose tissue was determined by the expression of endothelial marker CD31 using immunocytofluorescence. The endothelial-wise-induced cells expressed CD31 (Fig. 1E),

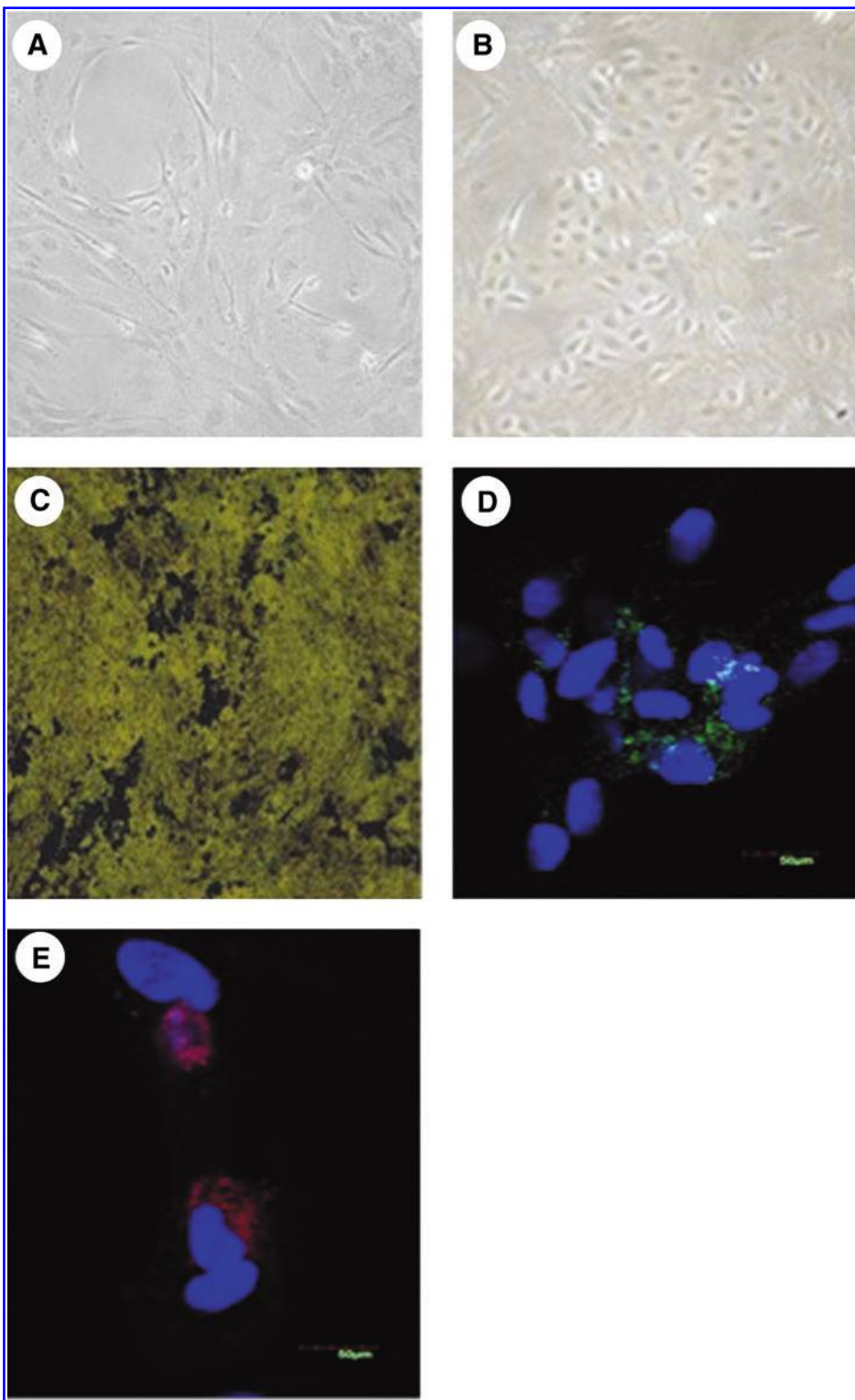


**FIG. 1.** Morphology and characterization of differentiated OBs and ECs. The OBs exhibited a spindle cell morphology (A), and the ECs exhibited a typical cobblestone morphology (B), magnification 20 $\times$ . Von Kossa staining visualized ossification nodules of induced OBs, indicating normal osteoblast function (C). The expression of osteocalcin was detected in osteogenic-wise induced cells (D). The expression of CD31 was detected in endothelial-wise induced cells (E). OBs, osteoblastic cells; ECs, endothelial cells. Color images available online at [www.liebertonline.com/tea](http://www.liebertonline.com/tea)

indicating the induced cells having a normal endothelial phenotype.

#### Gross examination

In total, 37 animals survived and completed the study: (1) no cells ( $n=9$ ); (2) undifferentiated ASC ( $n=8$ ); (3) adipose

tissue-derived OBs (Osteo,  $n=5$ ); (4) adipose tissue-derived ECs (Endo,  $n=7$ ); and (5) adipose tissue-derived OBs and ECs simultaneously (Osteo-Endo,  $n=8$ ). No evidence of infection, wound dehiscence, or implant extravasation occurred postoperatively or on harvesting of the calvarial implants after 8 weeks in the animals that completed the study.

### $\mu$ CT analysis

When quantifying the bone volume in the ROI through  $\mu$ CT, the amount of bone within the 8-mm defect area was significantly higher for the Endo group compared with both the Osteo and the Osteo-Endo groups ( $24.7 \pm 7.3 \text{ mm}^3$  vs.  $16.3 \pm 3.7 \text{ mm}^3$ ,  $p=0.05$  and  $16.6 \pm 5.7 \text{ mm}^3$ ,  $p=0.02$ , respectively) (Fig. 2). There were no significant differences in bone formation between the allografts treated with OBs alone ( $16.3 \pm 3.7 \text{ mm}^3$ ) or in combination with ECs ( $16.6 \pm 5.7 \text{ mm}^3$ ) and the allografts treated with no cells ( $19.6 \pm 2.8 \text{ mm}^3$ ) and undifferentiated ASC ( $20.5 \pm 4.3 \text{ mm}^3$ ).

In order to radiographically evaluate the degree of bone allograft integration at the allograft boundaries, the amount of bone volume within the 7-mm ROI was subtracted from the 8-mm ROI, which demonstrated no statistically significant differences in peripheral allograft integration among the treatment groups (No cells  $0.32 \pm 0.16 \text{ mm}^3$ ; undifferentiated ASC  $0.38 \pm 0.29 \text{ mm}^3$ ; Osteo  $0.33 \pm 0.3 \text{ mm}^3$ ; Endo  $0.47 \pm 0.15 \text{ mm}^3$ ; Osteo-Endo  $0.3 \pm 0.23 \text{ mm}^3$ ). In addition, when subtracting the amount of volume within the 8-mm ROI from the 9-mm ROI, there were no statistically significant differences among the groups, indicating a similar calvarial host bone resorption in all of them (No cells  $8.37 \pm 4.12 \text{ mm}^3$ ; undifferentiated ASC  $8.39 \pm 2.5 \text{ mm}^3$ ; Osteo  $4.72 \pm 3.92 \text{ mm}^3$ ; Endo  $4 \pm 2.14 \text{ mm}^3$ ; Osteo-Endo  $8.36 \pm 4.7 \text{ mm}^3$ ). With regard to the bone mineral density, there were no significant differences in bone mineral density among the groups (No cells  $1.29 \pm .04 \text{ g hydroxyapatite (HA)/cc}$ ; undifferentiated ASC  $1.29 \pm .07 \text{ g HA/cc}$ ; Osteo  $1.30 \pm .06 \text{ g HA/cc}$ ; Endo  $1.28 \pm .07 \text{ mg HA/cc}$ ; Osteo-Endo  $1.29 \pm .10 \text{ g HA/cc}$ ), as seen in Figure 3. Figure 4 shows a representative  $\mu$ CT of the implants at 8 weeks after implantation.

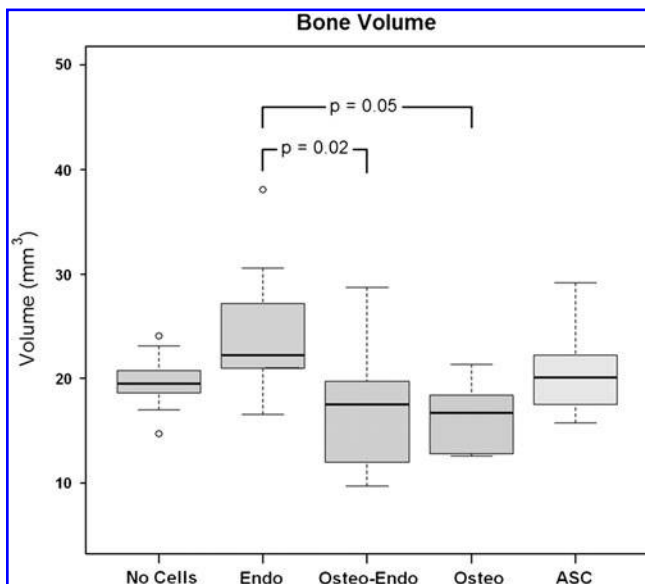


**FIG. 2.** Bone volume quantification measured in  $\mu\text{m}^3$  within the 8 mm allograft filled defect area at 8 weeks after implantation. The results were presented as median, 25% quartiles, and 75% quartiles; outliers are indicated by open dots. ASC, adipose tissue-derived stem cells.

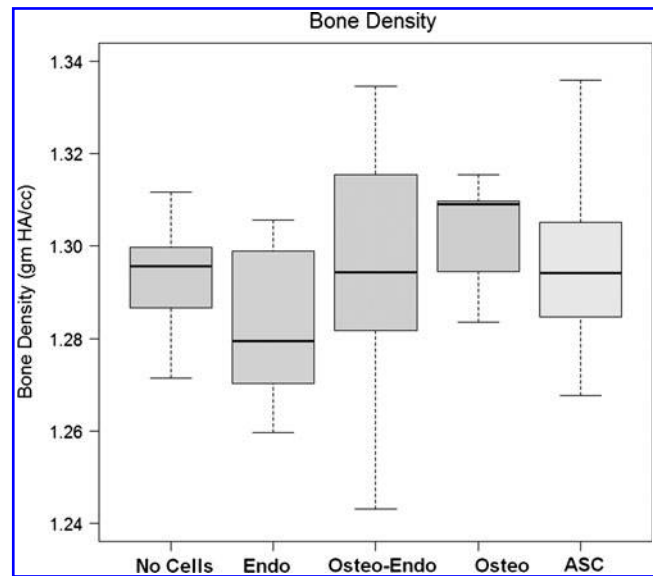


**FIG. 3.** Bone mineral density measured in gram HA/cc within the 8 mm allograft-filled defect area at 8 weeks after implantation. The results were presented as median, 25% quartiles, and 75% quartiles. HA, hydroxyapatite.

### Immunohistochemical evaluation

To confirm the contribution of ECs to vascularization of the implants, paraffin sections were immunohistochemically analyzed using rat-specific antibodies against the pan-endothelial marker CD34 (Fig. 5). The quantification of CD34-positive vessels in the central and peripheral areas of explanted allografts demonstrated a significantly higher amount of blood vessels in the implants treated with ECs alone ( $83.5 \pm 22.5 \text{ vessels/mm}^2$ ) relative to all groups (Fig. 6). In contrast, the implants in the Osteo-Endo group ( $34.7 \pm 21.8 \text{ vessels/mm}^2$ ) had relatively low amounts of blood vessels, similar to the implants in the Osteo group ( $36.3 \pm 16.2 \text{ vessels/mm}^2$ ). The amount of vessels in the control groups were  $45.1 \pm 12.9 \text{ vessels/mm}^2$  for the allografts without cells and  $45.8 \pm 7.0 \text{ vessels/mm}^2$  for the allografts treated with undifferentiated ASC.

### Discussion

The advantages of bone allograft recovered from deceased donor sources include its availability in various shapes and sizes, no donor-site morbidity, and avoidance of the need to sacrifice host structures. However, processed calvarial allogenic bone lacks osteogenic, osteoinductive, and angiogenic potential. These components are essential for successful graft healing and integration. In this project, we used *in vitro* predifferentiated rat ASC-derived ECs and OBs to investigate (1) whether treating cadaveric calvarial bone allografts with OBs and ECs independently improves their osteogenic and angiogenic potential, respectively, and (2) whether the coimplantation of these two cell lineages conveys a synergistic effect on bone allograft healing in a critical-sized orthotopic calvarial defect. We used an *in vivo* immunocompetent rat model, as it is a generally accepted model for allograft research<sup>12,24</sup> that can demonstrate the putative clinical application of engineered bone allografts.

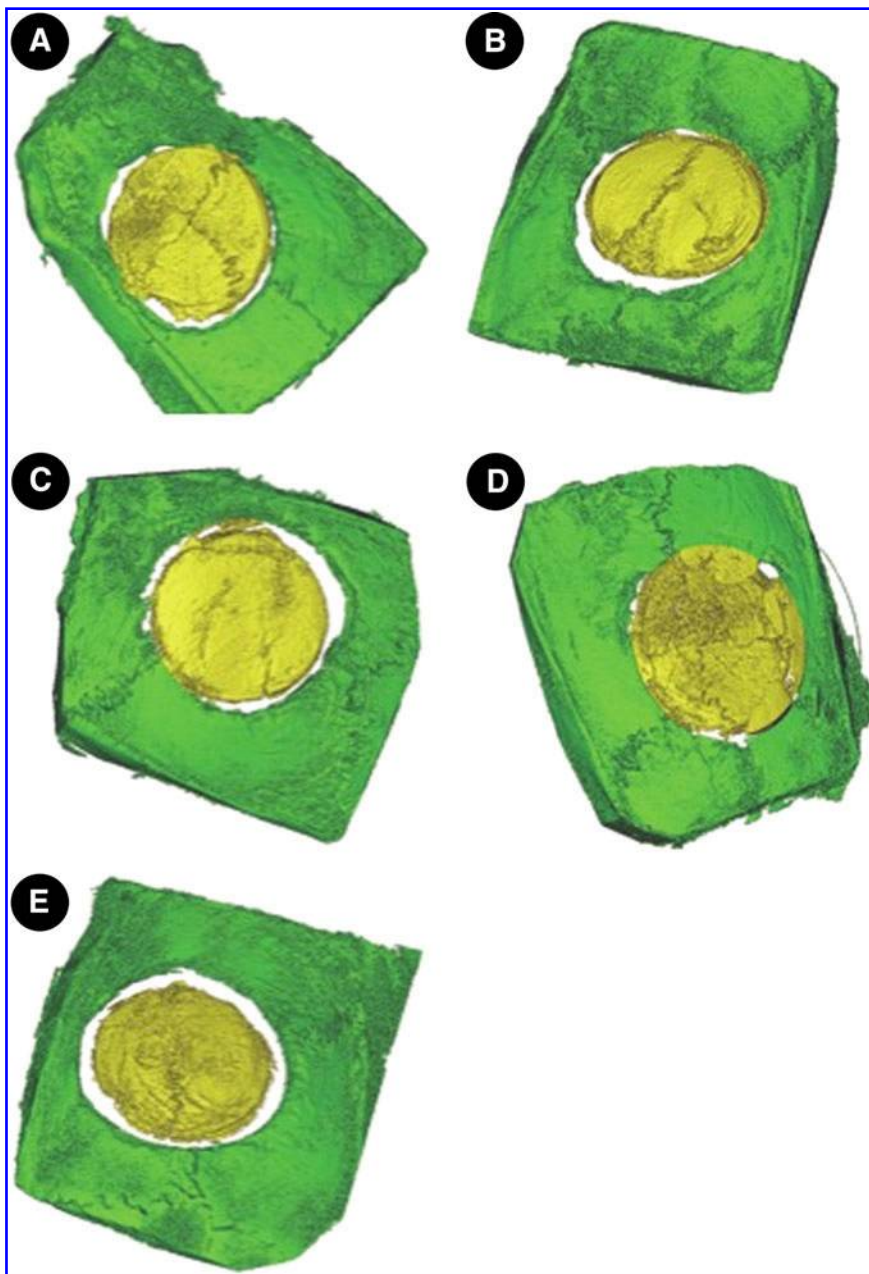


**FIG. 4.** Representative micro-computed tomography images of allograft-treated, critical-sized calvarial defects at 8 weeks after implantation. Allograft bone seeded with (A) no cells, (B) undifferentiated ASC, (C) adipose tissue-derived OBs, (D) adipose tissue-derived ECs, and (E) adipose tissue-derived OBs and ECs simultaneously. Color images available online at [www.liebertonline.com/tea](http://www.liebertonline.com/tea)

As hypothesized in our study, the implantation of ASC-derived ECs improved the vascularization within bone allograft implants at 8 weeks after treatment. This is demonstrated by the significantly higher microvessel density in the group treated with ECs relative to all groups. The angiogenic effect appeared to have a positive effect on osteogenesis, as demonstrated by the presence of greater bone volume in the allografts treated with ECs alone relative to all other groups. Of note, the Osteo and Osteo-Endo groups did not support bone formation, which is contrary to our second hypothesis.

Studies have demonstrated that ECs, regardless of their source or origin (adipose tissue, bone marrow, umbilical vein, or peripheral blood), have the potential to induce the formation of microvessels in engineered biomaterials without the need of exogenous growth factors.<sup>16,25–28</sup> This angiogenic effect is likely influenced by the up-regulation

of factors such as VEGF,<sup>29</sup> cytokines (e.g., granulocyte macrophage-colony stimulating factor or stromal cell derived factor-1),<sup>30,31</sup> and hormones such as estrogen,<sup>32</sup> which lead to the recruitment of ECs and accelerate angiogenesis.<sup>33</sup> In our study, we demonstrated that ASC-derived ECs alone are suitable as a vascularization strategy for allogenic bone implants, as evidenced by the significantly greater microvessel density in those allografts that received ECs compared with all groups (Fig. 6). Furthermore, the amount of bone was considerably higher in these allografts relative to the ones in the Osteo and Osteo-Endo groups (Fig. 2) and, thus, this finding suggests that at least during the early stage of bone formation, vascularity is essential and perhaps the most important factor in allograft healing.

Taking into consideration that the corresponding volume of the 8-mm×2-mm sized allograft is 100 mm<sup>3</sup>, our  $\mu$ CT

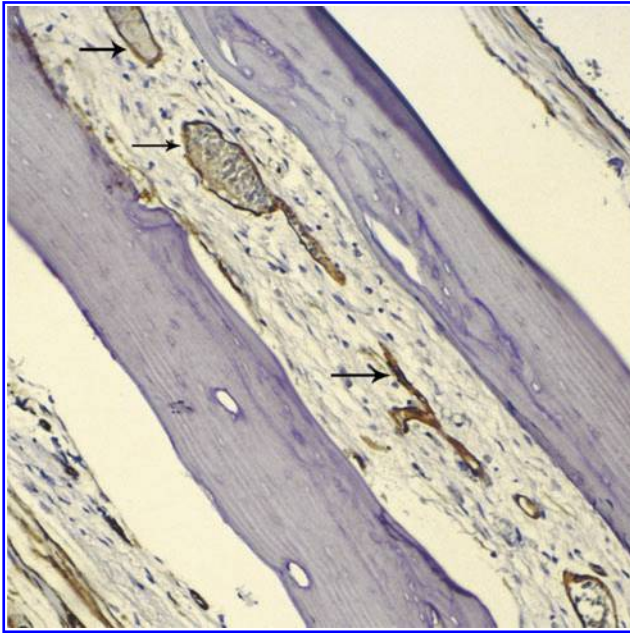


**FIG. 5.** Representative histological section showing blood vessels (arrows) immunostained with rat-specific CD34 antibody and counterstained with hematoxylin. Magnification 10 $\times$ . Color images available online at [www.liebertonline.com/tea](http://www.liebertonline.com/tea)

analysis demonstrated not only that the allografts treated with ECs had close to 25% (24.7 mm<sup>3</sup>) of bone present at 8 weeks, but also that bone formation did not happen at the expense of peripheral integration but throughout the allograft. In contrast, the healing of human bone allografts occurs mainly at the periphery with only 15% to 20% of allograft replaced with new bone after 5 years.<sup>34</sup> Both limi-

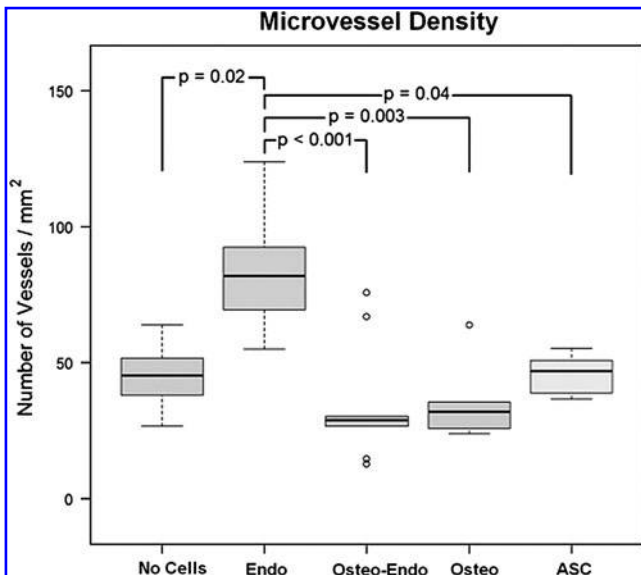


**FIG. 6.** The quantification of CD34-positive blood vessels demonstrated significantly more microvessels in the implants treated with ECs alone relative to all groups. The results were presented as median, 25% quartiles, and 75% quartiles; outliers are indicated by open dots.

tations have precluded their widespread use. In this regard, we recognize that in our study, the bone volume within the allografts is limited and, thus, the clinical relevance of this observation warrants further investigation.

One interesting observation is that the allografts in the Endo group were not treated with predifferentiated OBs and, thus, it is reasonable to assume that the bone formation in these constructs was secondary to the effect of invading host OBs or osteoprogenitor cells. In this context, it has been demonstrated that ECs contribute to bone formation by producing growth factors such as BMP-2, endothelin-1, and insulin-like growth factor, which can influence the proliferation of autogenous OBs and the differentiation of osteogenic precursor cells derived from the dura mater of the rats.<sup>16,35-37</sup> Furthermore, it is likely that the increased vascularization observed in these allografts improved oxygenation, nutrient delivery, and waste material removal, promoting an appropriate environment for local and invading cells to survive and function after implantation. This, in turn, can explain the presence of a greater bone volume in the allografts treated with ECs alone relative to all groups in our study.

The expected osteogenic effect in bone allografts treated with ASC-derived OBs and the synergistic effect of ASC-derived OBs and ECs in combination on bone allograft healing was not observed in this study. These results were in contrast to studies in various animal models that have demonstrated an enhanced osteogenic effect after treating bone allografts with adipose tissue or bone marrow-derived mesenchymal cells (MSCs) or OBs.<sup>13,14,38-40</sup> However, with the exception of the study by Lee *et al.*<sup>13</sup> where the allograft used was cortical diaphyseal bone treated with Gelfoam<sup>®</sup> containing bone marrow MSCs, most studies used cancellous bone allografts, which are intrinsically more porous and osteoinductive than cortical calvarial bone.<sup>41</sup> We used cortical bone in our experiment, because it provides strength and the ability to plate the bone in thereconstruction of large defects as opposed to cancellous bone, which is weaker and clinically more difficult to use in certain applications such as for long bone or mandible reconstruction.<sup>42</sup> Of note, in the study by Lee *et al.*, the authors recognized that it is difficult to incorporate MSCs into dense cortical bone and attributed their success to the creation of the effect of artificial periosteum made by Gelfoam.<sup>13</sup>

The porosity of a scaffold is considered a key element in bone tissue engineering, as it facilitates vascular and cellular invasion, which are crucial for cell viability after implantation.<sup>43</sup> Thus, the lack of porosity of the calvarial bone could have led to insufficient oxygen diffusion and vascular permeability within the allografts, which, in the absence of viable ECs that support an angiogenic response (as in the Endo group), compromised the viability of the transplanted OBs after implantation. In this regard, Follmar *et al.* reported similar results after treating cortical fibular bone allografts with ASC to repair large bone defects in rabbits and attributed their results to a lack of vascularization.<sup>44</sup> A study that further underscores the importance of adequate allograft perfusion was recently performed by Runyan *et al.*, who demonstrated an improved osteogenic effect in vascularized mandible allografts treated with ASC, whereas those with inferior vascularization showed increase resorption.<sup>34</sup>

The allografts in the Osteo-Endo group behaved similar to the allografts treated with OBs alone in terms of osteogenic and angiogenic activity, which further suggests that the

potential effect of ECs was not present in the coimplantation group. This result was in contrast to other reports where the coimplantation of ECs and OBs in engineered constructs demonstrated a synergistic osteogenic and vasculogenic effect in such cocultures compared with monocultures in three-dimensional synthetic biomaterials.<sup>16,19,21,26,27,35</sup> This result was also in contrast to recent findings by Koob *et al.*, who demonstrated a synergistic effect on neovessel formation in decalcified bovine cancellous bone allografts treated with ECs and MSCs in critical-sized defects.<sup>39</sup> It should be noted, however, that these studies have used different scaffold materials, bone defect models, and cell populations. In addition, some of these studies have used EPC, which have a greater doubling ability than mature ECs and display a higher potency to sprout out when cocultured with OBs.<sup>45–47</sup> Although there may be advantages to certain cell lineages, each may have different advantages in its clinical applicability and at present, the superiority of one cell line over another is yet to be established. In this study, we used ASC-derived OBs and ECs, because adipose tissue constitutes a very convenient cellular source, as it is relatively easy to obtain in large quantities, contains a large number of stromal stem cells, can be obtained in significantly greater quantities compared with the bone marrow or blood. Further studies comparing the yield of cells from different lineages may be helpful in elucidating the best model for use in the clinical setting.

Presently, it has not been entirely elucidated what ratio of OBs to ECs would be ideal to populate allogenic bone. Ma *et al.* recently reported that a 1:1 MSCs/ECs ratio is ideal to obtain osteogenic and angiogenic differentiation for cocultures *in vitro*.<sup>7</sup> In our experimental model, we used a 1:1 ratio of OBs and ECs, and in this case, we could not demonstrate a significant effect of either cell lineage. We chose this cell ratio in order to have equal influence by both cell lineages; however, recent studies suggest that a greater EC to OB cell ratio is necessary to successfully establish a viable construct with both cell lines. In this regard, Fuchs *et al.* cocultured OBs with ECs in a ratio of 3:2 onto silk fibroin scaffolds for approximately 4 weeks and demonstrated an increase from 60% to 89% in OBs and a decrease from 40% to 11.5% in ECs over time.<sup>19</sup> Recently, Unger *et al.* demonstrated that the ratios of ECs to OBs between 5:1 and 10:1 resulted in the presence of both cells types after one week on three-dimensional scaffolds, whereas the ratios of 1:1, 1:5, or 1:10 resulted in little or no ECs present after one week.<sup>16</sup> This result is supported by the findings of Koob *et al.*, who successfully induced an angiogenic effect by using a 5:1 ratio of ECs and OBs in allogenic bone implants.<sup>39</sup>

Although we did not employ a cell labeling method that tracks the fate of the implanted ECs, we suspect that a combination of the relatively low numbers of transplanted ECs which survived after coimplantation and the lack of scaffold porosity likely underlies the lack of a significant osteogenic effect in this group. It is possible that the evaluation of osteogenesis at later time points may yield different results, given that bone allografts are intrinsically osteoconductive and with time undergo bone formation through creeping substitution or the migration of host osteogenic cellular elements. Likewise, it is possible to observe changes in allograft vascularization that can occur through a complex host-derived mechanism mediated by cytokines, adjacent

cell interactions, and proteolytic enzymes that modify regulatory molecules, cell surface molecules, and the extracellular matrix.<sup>2</sup>

Although we were able to improve the vascularization in bone allografts, therapeutic approaches that improve other major biological deficiencies, those being lack of osteogenicity and osteoinduction, are still needed. Recently, advances in gene delivery techniques have made possible the use of BMPs in combination with osteogenic cells to treat bone allografts with encouraging results in allograft healing and integration.<sup>5,34,48,49</sup> A combination of these therapies is a promising strategy that improves the osteogenic and osteoinductive potential of structural bone allografts.

In summary, our results show that the implantation of ASC-derived ECs improves the vascularization within bone allografts at 8 weeks after treatment *in vivo*. Our findings support a growing body of evidence in support of cell-based therapies using ECs to improve the vascularity of engineered bone constructs.

### Acknowledgment

This work was supported by a grant from the National Endowment for Plastic Surgery.

### Disclosure Statement

No competing financial interests exist.

### References

- Schroeder, J.E., and Mosheiff, R. Tissue engineering approaches for bone repair: concepts and evidence. *Injury* **42**, 609, 2011.
- Bishop, A.T., and Pelzer, M. Vascularized bone allotransplantation: current state and implications for future reconstructive surgery. *Orthop Clin North Am* **38**, 109, 2007.
- Enneking, W.F., and Campanacci, D.A. Retrieved human allografts: a clinicopathological study. *J Bone Joint Surg Am* **83-A**, 971, 2001.
- Li, Y., Shi, S., Li, Q., Wang, Z., Hu, Y., Lu, R., Liu, X., Ji, X., Zhu, B., and Ding, H. [Fate of massive retrieved human bone allografts]. *Zhonghua Wai Ke Za Zhi* **36**, 169, 1998.
- Di Bella, C., Aldini, N.N., Lucarelli, E., Dozza, B., Frisoni, T., Martini, L., Fini, M., and Donati, D. Osteogenic protein 1 associated with mesenchymal stem cells promote bone allograft integration. *Tissue Eng Part A* **16**, 2967, 2010.
- Griffith, C.K., Miller, C., Sainson, R.C., Calvert, J.W., Jeon, N.L., Hughes, C.C., and George, S.C. Diffusion limits of an *in vitro* thick prevascularized tissue. *Tissue Eng* **11**, 257, 2005.
- Ma, J., van den Beucken, J.J., Yang, F., Both, S.K., Cui, F.Z., Pan, J., and Jansen, J.A. Coculture of osteoblasts and endothelial cells: optimization of culture medium and cell ratio. *Tissue Eng Part C Methods* **17**, 349, 2011.
- Zuk, P.A., Zhu, M., Mizuno, H., Huang, J., Futrell, J.W., Katz, A.J., Benhaim, P., Lorenz, H.P., and Hedrick, M.H. Multilineage cells from human adipose tissue: implications for cell based therapies. *Tissue Eng* **7**, 211, 2001.
- Bunnell, B.A., Flaat, M., Gagliardi, C., Patel, B., and Ripoll, C. Adipose derived stem cells: isolation, expansion and differentiation. *Methods* **45**, 115, 2008.
- Fink, T., Rasmussen, J.G., Lund, P., Pilgaard, L., Soballe, K., and Zachar, V. Isolation and expansion of adipose derived stem cells for tissue engineering. *Front Biosci (Elite Ed)* **3**, 256, 2011.

11. Sterodimas, A., de Faria, J., Nicaretta, B., and Pitanguy, I. Tissue engineering with adipose derived stem cells (ADSCs): current and future applications. [J Plast Reconstr Aesthet Surg](#) **63**, 1886, 2010.
12. Bohnenblust, M.E., Steigelman, M.B., Wang, Q., Walker, J.A., and Wang, H.T. An experimental design to study adipocyte stem cells for reconstruction of calvarial defects. [J Craniofac Surg](#) **20**, 340, 2009.
13. Lee, J.Y., Choi, M.H., Shin, E.Y., and Kang, Y.K. Autologous mesenchymal stem cells loaded in Gelfoam((R)) for structural bone allograft healing in rabbits. [Cell Tissue Bank](#) **12**, 299, 2011.
14. Li, Z., and Li, Z.B. Repair of mandible defect with tissue engineering bone in rabbits. [ANZ J Surg](#) **75**, 1017, 2005.
15. Abukawa, H., Shin, M., Williams, W.B., Vacanti, J.P., Kaban, L.B., and Troulis, M.J. Reconstruction of mandibular defects with autologous tissue engineered bone. [J Oral Maxillofac Surg](#) **62**, 601, 2004.
16. Unger, R.E., Sartoris, A., Peters, K., Motta, A., Migliaresi, C., Kunkel, M., Bulnheim, U., Rychly, J., and Kirkpatrick, C.J. Tissue like self assembly in cocultures of endothelial cells and osteoblasts and the formation of microcapillary like structures on three dimensional porous biomaterials. [Bio materials](#) **28**, 3965, 2007.
17. Ito, H., Koefoed, M., Tiyyapanaputi, P., Gromov, K., Goater, J.J., Carmouche, J., Zhang, X., Rubery, P.T., Rabinowitz, J., Samulski, R.J., Nakamura, T., Soballe, K., O'Keefe, R.J., Boyce, B.F., and Schwarz, E.M. Remodeling of cortical bone allografts mediated by adherent rAAV RANKL and VEGF gene therapy. [Nat Med](#) **11**, 291, 2005.
18. Hanjaya Putra, D., and Gerecht, S. Vascular engineering using human embryonic stem cells. [Biotechnol Prog](#) **25**, 2, 2009.
19. Fuchs, S., Hofmann, A., and Kirkpatrick, C.J. Microvessel like structures from outgrowth endothelial cells from human peripheral blood in 2 dimensional and 3 dimensional cocultures with osteoblastic lineage cells. [Tissue Eng](#) **13**, 2577, 2007.
20. Levenberg, S., Rouwkema, J., Macdonald, M., Garfein, E.S., Kohane, D.S., Darland, D.C., Marini, R., van Blitterswijk, C.A., Mulligan, R.C., D'Amore, P.A., and Langer, R. Engineering vascularized skeletal muscle tissue. [Nat Biotechnol](#) **23**, 879, 2005.
21. Rouwkema, J., de Boer, J., and Van Blitterswijk, C.A. Endothelial cells assemble into a 3 dimensional prevascular network in a bone tissue engineering construct. [Tissue Eng](#) **12**, 2685, 2006.
22. Rouwkema, J., Westerweel, P.E., de Boer, J., Verhaar, M.C., and van Blitterswijk, C.A. The use of endothelial progenitor cells for prevascularized bone tissue engineering. [Tissue Eng Part A](#) **15**, 2015, 2009.
23. Seebach, C., Schultheiss, J., Wilhelm, K., Frank, J., and Henrich, D. Comparison of six bone graft substitutes regarding to cell seeding efficiency, metabolism and growth behaviour of human mesenchymal stem cells (MSC) *in vitro*. [Injury](#) **41**, 731, 2010.
24. Francis, P.O., McPherson, J.C., 3rd, Cuenin, M.F., Hokett, S.D., Peacock, M.E., Billman, M.A., and Sharawy, M. Evaluation of a novel alloplast for osseous regeneration in the rat calvarial model. [J Periodontol](#) **74**, 1023, 2003.
25. Fedorovich, N.E., Haverslag, R.T., Dhert, W.J., and Alblas, J. The role of endothelial progenitor cells in prevascularized bone tissue engineering: development of heterogeneous constructs. [Tissue Eng Part A](#) **16**, 2355, 2010.
26. Scherberich, A., Galli, R., Jaquiere, C., Farhadi, J., and Martin, I. Three dimensional perfusion culture of human adipose tissue derived endothelial and osteoblastic progenitors generates osteogenic constructs with intrinsic vascularization capacity. [Stem Cells](#) **25**, 1823, 2007.
27. Yu, H., Vandevord, P.J., Gong, W., Wu, B., Song, Z., Matthew, H.W., Wooley, P.H., and Yang, S.Y. Promotion of osteogenesis in tissue engineered bone by pre seeding endothelial progenitor cells derived endothelial cells. [J Orthop Res](#) **26**, 1147, 2008.
28. Borges, J., Mueller, M.C., Padron, N.T., Tegtmeier, F., Lang, E.M., and Stark, G.B. Engineered adipose tissue supplied by functional microvessels. [Tissue Eng](#) **9**, 1263, 2003.
29. Asahara, T., Takahashi, T., Masuda, H., Kalka, C., Chen, D., Iwaguro, H., Inai, Y., Silver, M., and Isner, J.M. VEGF contributes to postnatal neovascularization by mobilizing bone marrow derived endothelial progenitor cells. [EMBO J](#) **18**, 3964, 1999.
30. Takahashi, T., Kalka, C., Masuda, H., Chen, D., Silver, M., Kearney, M., Magner, M., Isner, J.M., and Asahara, T. Ischemia and cytokine induced mobilization of bone marrow derived endothelial progenitor cells for neovascularization. [Nat Med](#) **5**, 434, 1999.
31. Yamaguchi, J., Kusano, K.F., Masuo, O., Kawamoto, A., Silver, M., Murasawa, S., Bosch Marce, M., Masuda, H., Losordo, D.W., Isner, J.M., and Asahara, T. Stromal cell derived factor 1 effects on *ex vivo* expanded endothelial progenitor cell recruitment for ischemic neovascularization. [Circulation](#) **107**, 1322, 2003.
32. Strehlow, K., Werner, N., Berweiler, J., Link, A., Dirnagl, U., Priller, J., Laufs, K., Ghaeni, L., Milosevic, M., Bohm, M., and Nickenig, G. Estrogen increases bone marrow derived endothelial progenitor cell production and diminishes neointima formation. [Circulation](#) **107**, 3059, 2003.
33. Kaully, T., Kaufman Francis, K., Lesman, A., and Levenberg, S. Vascularization the conduit to viable engineered tissues. [Tissue Eng Part B Rev](#) **15**, 159, 2009.
34. Runyan, C.M., Jones, D.C., Bove, K.E., Maercks, R.A., Simpson, D.S., and Taylor, J.A. Porcine allograft mandible revitalization using autologous adipose derived stem cells, bone morphogenetic protein 2, and periosteum. [Plast Reconstr Surg](#) **125**, 1372, 2010.
35. Kaigler, D., Krebsbach, P.H., West, E.R., Horger, K., Huang, Y.C., and Mooney, D.J. Endothelial cell modulation of bone marrow stromal cell osteogenic potential. [FASEB J](#) **19**, 665, 2005.
36. Ozerdem, O.R., Anlatici, R., Bahar, T., Kayaselcuk, F., Barutcu, O., Tuncer, I., and Sen, O. Roles of periosteum, dura, and adjacent bone on healing of cranial osteonecrosis. [J Craniofac Surg](#) **14**, 371, 2003.
37. Warren, S.M., Greenwald, J.A., Nacamuli, R.P., Fong, K.D., Song, H.J., Fang, T.D., Mathy, J.A., and Longaker, M.T. Regional dura mater differentially regulates osteoblast gene expression. [J Craniofac Surg](#) **14**, 363, 2003.
38. Tang, T.T., Lu, H., and Dai, K.R. Osteogenesis of freeze dried cancellous bone allograft loaded with autologous marrow derived mesenchymal cells. [Mater Sci Eng](#) **20**, 57, 2002.
39. Koob, S., Torio Padron, N., Stark, G.B., Hannig, C., Stankovic, Z., and Finkenzeller, G. Bone formation and neovascularization mediated by mesenchymal stem cells and endothelial cells in critical sized calvarial defects. [Tissue Eng Part A](#) **17**, 311, 2011.
40. Schubert, T., Xhema, D., Vériter, S., Schubert, M., Behets, C., Delloye, C., Gianello, P., and Dufrane, D. The enhanced

- performance of bone allografts using osteogenic differentiated adipose derived mesenchymal stem cells. *Biomaterials* **32**, 8880, 2011.
41. Marins, L.V., Cestari, T.M., Sottovia, A.D., Granjeiro, J.M., and Taga, R. Radiographic and histological study of perianal bone defect repair in rat calvaria after treatment with blocks of porous bovine organic graft material. *J Appl Oral Sci* **12**, 62, 2004.
  42. Wallace, C.G., Chang, Y.M., Tsai, C.Y., and Wei, F.C. Harnessing the potential of the free fibula osteoseptocutaneous flap in mandible reconstruction. *Plast Reconstr Surg* **125**, 305, 2010.
  43. Sicchieri, L.G., Crippa, G.E., de Oliveira, P.T., Beloti, M.M., and Rosa, A.L. Pore size regulates cell and tissue interactions with PLGA CaP scaffolds used for bone engineering. *J Tissue Eng Regen Med* **6**, 155, 2012.
  44. Follmar, K.E., Prichard, H.L., DeCroos, F.C., Wang, H.T., Levin, L.S., Klitzman, B., Olbrich, K.C., and Erdmann, D. Combined bone allograft and adipose derived stem cell autograft in a rabbit model. *Ann Plast Surg* **58**, 561, 2007.
  45. Seebach, C., Henrich, D., Kahling, C., Wilhelm, K., Tami, A.E., Alini, M., and Marzi, I. Endothelial progenitor cells and mesenchymal stem cells seeded onto beta TCP granules enhance early vascularization and bone healing in a critical sized bone defect in rats. *Tissue Eng Part A* **16**, 1961, 2010.
  46. Lin, Y., Weisdorf, D.J., Solovey, A., and Hebbel, R.P. Origins of circulating endothelial cells and endothelial outgrowth from blood. *J Clin Invest* **105**, 71, 2000.
  47. Stahl, A., Wu, X., Wenger, A., Klagsbrun, M., and Kurschat, P. Endothelial progenitor cell sprouting in spheroid cultures is resistant to inhibition by osteoblasts: a model for bone replacement grafts. *FEBS Lett* **579**, 5338, 2005.
  48. Hsu, W.K., Sugiyama, O., Park, S.H., Conduah, A., Feeley, B.T., Liu, N.Q., Krenek, L., Virk, M.S., An, D.S., Chen, I.S., and Lieberman, J.R. Lentiviral mediated BMP 2 gene transfer enhances healing of segmental femoral defects in rats. *Bone* **40**, 931, 2007.
  49. Xie, C., Reynolds, D., Awad, H., Rubery, P.T., Pelled, G., Gazit, D., Guldberg, R.E., Schwarz, E.M., O'Keefe, R.J., and Zhang, X. Structural bone allograft combined with genetically engineered mesenchymal stem cells as a novel platform for bone tissue engineering. *Tissue Eng* **13**, 435, 2007.

Address correspondence to:  
Howard T Wang, M.D.

Division of Plastic and Reconstructive Surgery  
University of Texas Health Science Center at San Antonio  
7703 Floyd Curl Drive  
San Antonio, TX 78229-3900

E-mail: wanght@uthscsa.edu

Received: September 11, 2011

Accepted: March 16, 2012

Online Publication Date: May 10, 2012

**This article has been cited by:**

1. Michael D. Hoffman, Danielle S. W. Benoit. 2012. Emerging Ideas: Engineering the Periosteum: Revitalizing Allografts by Mimicking Autograft Healing. *Clinical Orthopaedics and Related Research*## . [[CrossRef](#)]